Article

Multifunctional Probe Based on Cationic Conjugated Polymers for Nitroreductase- Related Analysis: Sensing, Hypoxia Diagnosis and Imaging

Xiaoqian Zhang, Qi Zhao, Yanru Li, Xinrui Duan, and Yanli Tang

Anal. Chem., **Just Accepted Manuscript** • Publication Date (Web): 19 Apr 2017

Multifunctional Probe Based on Cationic Conjugated Polymers for Nitroreductase-Related Analysis: Sensing, Hypoxia Diagnosis and Imaging

Xiaoqian Zhang, Qi Zhao, Yanru Li, Xinrui Duan, Yanli Tang*

Key Laboratory of Analytical Chemistry for Life Science of Shaanxi Province, Key Laboratory of Applied Surface and Colloid Chemistry, Ministry of Education, School of Chemistry and Chemical Engineering, Shaanxi Normal University, Xi'an 710062, P. R. China

[*]E-mail: yltang@snnu.edu.cn. Fax: (086) 29-81530727 (Prof. Y. L. Tang)

ABSTRACT: Nitroreductase (NTR) is overexpressed in hypoxic tumors. Moreover, hypoxia is usually considered as a most important feature of various diseases. Thus it is important to build a sensitive and selective method for NTR detection and hypoxia diagnosis. Herein, a new cationic conjugated polymer (PBFBT-NP) with p-nitrophenyl group in the side chain was designed and synthesized as a fluorescent probe for the detection of NTR. In the absence of NTR, the fluorescence of PBFBT-NP was quenched due to photo-induced electron transfer (PET). On the contrary, in the presence of NTR, NTR can specifically react with p-nitrophenyl group to form p-aminophenyl group, which leads to the PET being inhibited and the polymer's fluorescence thus significantly increasing (>110-fold). The sensitive and selective NTR sensing method in vitro is thus constructed with a low detection limit of 2.9 ng/mL. Moreover, the hypoxic status of tumor cells can be visualized by fluorescence bioimaging with very low cytotoxicity. Interestingly, the probe was successfully used for imaging NTR-expressed microorganism, such as *E. coli*, and showed excellent antibacterial activity against *E. coli* under white light irradiation. In brief, this multifunctional probe is promising for widespread use in NTR-related biological analysis.

KEYWORDS: Cationic conjugated polymers; Nitroreductase detection; Hypoxia diagnosis; Photo-induced electron transfer; Bioimaging

INTRODUCTION

Hypoxia refers to a state in which oxygen supply is insufficient, which is usually considered as a most important feature of various diseases, including acute cerebrovascular disease, cardiac ischemia, stroke, inflammatory diseases and the solid tumors. Clinical researches indicated that the hypoxic status of tumors is closely related with tumor progression toward a more malignant phenotype with increased metastatic potential.[1-4] Moreover, hypoxia cells can reduce the efficiency of anti-cancer drugs to some degree compared with normoxic cells.[5-9] Therefore, the estimation of tumor hypoxia degree is very important for predicting anticancer efficacies. Because of this, it remains urgently vital to develop a novel approach to detect hypoxia status selectively and sensitively. It is known that the reductive enzymes, including nitroreductase (NTR), azoreductase and quinone reductase, are overexpressed in hypoxia status cells.[3,4,7] Among them, NTR is considered as an indicative biomarker because NTR level corresponds directly with the degree of hypoxia.[10-15] Therefore, the hypoxia status in a tumor can be directly assessed by detecting the level of NTR.

Nitroreductase, a cytosolic enzyme, can make use of NADH or NADPH as an electron source to reduce the nitro groups to the corresponding amines.[16-18] Recently, several new techniques based on fluorescent probes have been designed for NTR detection.[2,7,12,18,19-28] Among them, fluorescent probes based

on nitroaromatic compounds are obtained widely attention because of their high sensitivity, selectivity and in situ detection. However, most of them require long response time, tedious procedures, expensive instruments or materials, and poor water solubility, which limit their practical applications. [2,7,12,18,19-22,25-28]

In recent years, cationic conjugated polymers (CCPs), comprised of a large number of conjugated repeat units, have gained more and more attention due to their unique photo- and electro-characteristics.[29-37] Upon irradiation by ultraviolet (UV) or visible light, exciton can be efficiently transferred to a lower electron or energy acceptor sites along the whole backbone of the conjugated polymer, which gives rise to fluorescent signal amplification.[38-40] Modification with different functional groups on side-chains of CCPs can allow CPPs to specifically detect a series of targets, such as, enzymes, oligonucleotides, toxic metal ions, and so on. Therefore, these favorable advantages make CCPs applicable in biosensors and cell imaging, etc.[41-45]

Inspired by the characteristics of CCPs and biological effects of NTR, a new "turn-on" fluorescent CCPs probe PBFBT-NP was synthesized to detect NTR. PBFBT-NP probe has good water-solubility and contain nitro group which specifically reacts with NTR. It was reported that aromatic nitro group, as strong electron-withdrawing group, could modulate the fluorescence properties of fluorophore via a photoinduced electron transfer (PET) process from the excited fluorophore to aromatic nitro group.[7, 46] When the nitro group was

introduced to PBFBT-NP on the side chains, it is reasonably to assume that the fluorescence of PBFBT-NP is quenched through PET from the backbones to the side chains (Scheme 1). However, when NTR is present, which reduces the nitro to amine group, PET could be efficiently blocked followed by PBFBT-NPemitting strong fluorescence. Thus this strategy provides us a sensitive and simple method to detect NTR and NTR-related hypoxia diagnosis. Moreover, it is known that NTR is usually expressed in microorganism, such as *Escherichia coli*. The new probe also can be used for bacteria imaging without the use of expensive commercial stain and used for antibacterial agent.

EXPERIMENTAL SECTION

Materials and Measurements. All chemicals were purchased from J&K Scientific Ltd. (Beijing, China), Aladdin Industrial Corporation (Shanghai, China) or Sinopharm chemical reagent Co. Ltd. (Beijing, China), and were used without any further purification. Nitroreductase from *E. coli* was purchased from Sigma-Aldrich Co. Ltd. (St. Louis, MO, USA). β-Nicotinamide adenine dinucleotide disodium salt hydrate (NADH) was purchased from TCI Co. Ltd. (Shanghai, China). The anaerobic culture bags were purchased from Mitsubishi gas chemical Co. Ltd. (Tokyo, Japan). Ultrapure water was collected from a Milli-Q reference system. All pH measurements were carried out with a Sartorius basic pH-Meter. UV-vis absorption spectra were taken on a Perkin Elmer Lambda 35 spectrophotometer. The fluorescence spectra were recorded on a Hitachi F-7000 spectrophotometer equipped with a xenon lamp

excitation source. Fluorescence imaging experiments of *E. coli* were performed on an Olympus IX73; Confocal laser scanning microscopy images of A549 cells were recorded on Olympus Fluo-view 1200. Copolymer molecular weight was measured by GPC-MALLS. The antibacterial activities were recorded using an Accuri C6 flow cytometry. TEM images were obtained using Tecnai G2 F20 Field Transmission Electron Microscopy (FEI). ^{1}H NMR and ^{13}C NMR spectra were recorded on Bruker Avance 300 MHz and Ascend 600 MHz spectrometers.

Synthesis of Monomer 3. Under nitrogen, p-nitrophenol (0.696 g, 5 mmol) and NaH (0.12 g, 5 mmol) were dissolved in DMF (30 mL). After stirring at room temperature for 15 min, compound 2 (0.389 g, 0.782 mmol) was added to the mixed solution and then stirred at room temperature for 24 h. The final mixture was extracted with CH_2Cl_2 and the collected organic phase was washed with HCl solution (1 M), brine and distilled water, and then dried over $MgSO_4$ and concentrated under vacuum. The residue was subjected to silica gel chromatography, eluted with petroleum ether/ ethyl acetate (v/v=16:1), affording **monomer 3** (0.121 g, 28%) as yellow solid**.** ^{1}H NMR (300 MHz, $CDCl_3$), δ 8.22 (d, J = 9.0 Hz, 2 H), 7.22 (s, 1 H), 7.17 (s, 1 H), 7.01 (d, J = 9.0 Hz, 2 H), 4.35 (t, J = 6.0 Hz, 2 H), 4.15 (t, J = 6.0 Hz, 2 H), 3.82 (s, 3 H), 2.33(m, 2 H). ^{13}C NMR (75 MHz, $CDCl_3$) δ 163.9, 153.7, 152.4, 141.6, 125.9, 123.2, 121.4, 114.5, 85.5, 65.23, 57.2, 29.0. HRMS (ESI): m/z: calcd. for $C_{16}H_{15}I_2NO_5$ Na^+ 577.8938$[M+Na]^+$, found 577.8938 $[M+Na]^+$.

Synthesis of Br-PBFBT-NP. Monomer 1 (71.68 mg, 0.110 mmol), **monomer 2**

(117.22 mg, 0.158 mmol), **monomer 3** (8.74 mg, 0.0158 mmol), 4,7-dibromo-2,1,3-benzothiadiazole (9.26 mg, 0.0315 mmol), THF (20 mL) and K_2CO_3 solution (2 M, 10 mL) were mixed and degassed with nitrogen gas for 30 min. $PdCl_2$(dppf) (36.60 mg, 0.05 mmol) was then added to the solution at room temperature under nitrogen. The mixed solution was heated at 85 ^oC for 48 h. The cooled mixture was extracted with $CHCl_3$, washed with distilled water, dried over Na_2SO_4 and concentrated under vacuum. The residue was dissolved in $CHCl_3$ and precipitated in methanol 3 times to give Br-PBFBT-NP as black solid (80 mg, 57%). ^1H NMR (300 MHz, $CDCl_3$), δ 8.01-7.38 (m), 7.11 (m), 6.85 (m), 4.21 (br), 4.06 (br), 3.87 (br), 3.30 (br), 3.08 (br), 2.15 (br), 1.69 (br), 1.25 (br), 0.88 (br). GPC-MALLS: Mw=24,215; Mn=14,679; PDI=1.65 (The solvent is THF).

Synthesis of PBFBT-NP. Br-PBFBT-NP (30 mg) was dissolved in $CHCl_3$ (45 mL) and the reaction mixture was stirred vigorously to form a homogeneous solution. Then, trimethylamine ethanol solution (2 mL) was added and the mixture was stirred at room temperature for 72 h. The solid was collected by filtration, washed with $CHCl_3$ 3 times and dried under vacuum to give **PBFBT-NP** as black solid (29 mg, 79% (molar yield)). ^1H NMR (600 MHz, MeOD), δ 8.09-7.38 (m), 4.29 (t), 4.08 (m), 3.65 (s), 3.28 (m), 3.06 (br), 2.19 (br), 1.60 (br), 1.29 (br), 0.90 (br).

General Procedure for NTR Detection. In 2.0 mL Tris-HCl (10 mM, pH 7.4) solution, 0.1 μM (final concentration) PBFBT-NP and 100 μM (final concentration) NADH were added. Then, NTR was added and incubated at 37 ^oC. Fluorescence

spectra were recorded with the excitation wavelength of 430 nm. Under the same conditions, the blank solution (without nitroreductase) was prepared and measured.

Cell Culture. The A549 cells were grown in dulbecco's modified eagle's medium (DMEM) supplemented with 10% fetal bovine serum (FBS) and cultured at 37 °C under 5% CO_2 for normoxic condition (20% O_2), otherwise A549 cells were cultured for 6 h at 37 °C under anaerobic conditions.

Strain and Growth Condition. Gram-negative bacteria *E. coli* as model bacteria was used in this study. Bacterial samples were transferred from the frozen state onto agar slants (1.2% agar + Lysogeny Broth (LB) for E. coli) and incubated at 37 ^{o}C overnight and then held at 4 ^{o}C for up to 2 weeks. Every time, a colony of bacteria was put on LB (20 mL) and cultured at 37 ^{o}C overnight. After growth, the bacterial culture was centrifuged at 6000 rpm/min three times. Then the pellet was suspended in 0.9% NaCl solution. The final concentration of bacteria was around 2×10^7 mL^{-1}.

RESULTS AND DISCUSSION

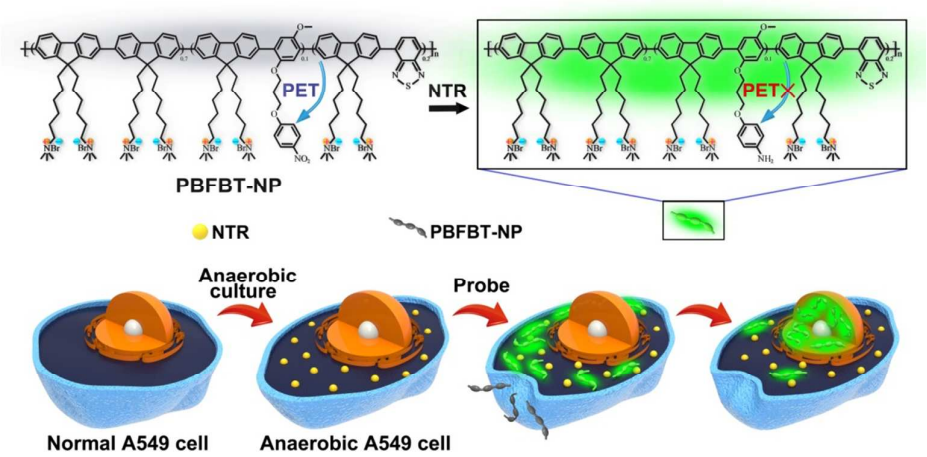

Scheme 1 The schematic presentation of the nitro group reduced into the amino group by NTR and cell hypoxia diagnosis.

Design and Synthesis of PBFBT-NP. The important features of suitable fluorescent probes for NTR detection should have enhanced fluorescence, fast and sensitive response, good selectivity. Taking all of these characteristics into account, we designed and synthesized the copolymer PBFBT-NP probe by a Suzuki coupling reaction between monomer 1, 2, 3 and 4,7-dibromo-2,1,3 -benzothiadiazole and the following quaternization reaction, which meets the requirement that a fluorescent probe should consist of a detecting part and a fluorescence reporting part. Herein, the monomer 1/2 with quaternary ammonium groups linked to the side chains makes PBFBT-NP possessing excellent water-solubility, monomer 3 makes PBFBT-NP detecting NTR selectively, and 4,7-dibromo-2,1,3-benzothiadiazole makes PBFBT-NP having a absorption wavelength in visible light range.[30,50-51] Structurally, p-nitrophenol was covalently linked to the side chain of PBFBT-NP, which is not only served as an electron acceptor (a fluorescence quencher) but also as a NTR trapper. In fact, due to p-nitrophenyl side groups playing key roles in target recognition and fluorescence quenching, the proportion of p-nitrophenyl side groups has important influence on the NTR sensing. If the proportion of groups is too small, the fluorescence from main chains could not be quenched effectively, which will increase the background signal. Otherwise, if the proportion of

groups is too large, the fluorescence can be quenched effectively, but to enhance the fluorescence it requires more NTR to react with the groups. Taking these points in account, we chose the proportion as 0.1 to prepare the probe that presented a very low background signal and an excellent response to NTR. The main chains of conjugated polymers are fluorescence reporting part.

The synthesis of PBFBT-NP was illustrated in Scheme 2. Compound 1,[47] monomer 1 and 2[48-49] were synthesized according to the literatures. Reaction of compound 2 with p-nitrophenol affords monomer 3. The Br-PBFBT-NP is prepared by a Suzuki coupling reaction between monomer 1, 2, 3 and 4,7-dibromo-2,1,3-benzothiadiazole in the presence of $PdCl_2$(dppf) in THF and K_2CO_3 solution. Then cationic PBFBT-NP is obtained by quaternarization reaction of the precursor Br-PBFBT-NP (Figure S10) with trimethylamine in $CHCl_3$. As shown in Figure S10 and Figure S11, the NMR peak attribution was presented for every spectrum in details. In Figure S10, the peak at 4.06 and 3.30 belong to -CH_2 (C-127) in Monomer 3 side chain and -CH_2Br in Monomer 1/2 side chain, respectively. According to the integral ratio, one can estimate Monomer 1 and 2 to Monomer 3 ratio is around 7:1. As shown in Figure S11, after quaternization, the peak at 3.06 and 2.19 belong to -$N(CH_3)_3$Br and -CH_2 in Monomer 1/2 side chain, respectively. Furthermore, the ratio between them is around 3, which means the quaternization efficiency is about 66%. Due to the overlay of hydrogen chemical shift on aromatic rings, it is difficult to determine

the actual ratio of 4,7-dibromo-2,1,3-benzothiadiazole. Therefore, we still used the theoretical ratio as the proportion of monomer in the copolymer. Because of copolymers with high molecular weight, it is not easy to obtain a higher concentration in D_2O to meet the requirement for NMR measurement. Because PBFBT-NP copolymers are amphiphilic macromolecules, when they are soluble in water, the copolymers may form very loose aggregates that could be affected easily by microenvironment. The size distribution measurement was conducted by the dynamic light scattering (DLS). As shown in Figure S1, the size is around 161 ± 18 nm. TEM image showed copolymers formed nanoparticles, which is coincident with the DLS data.

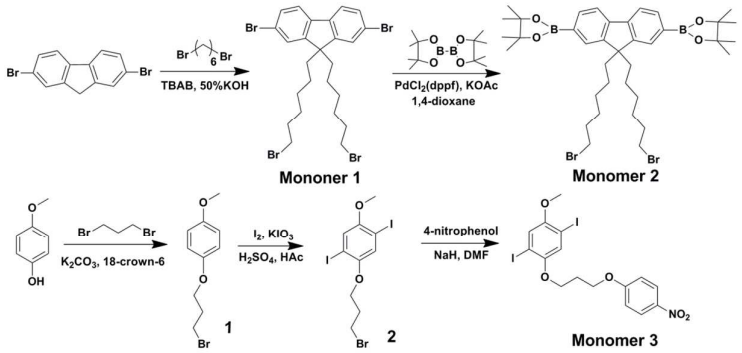

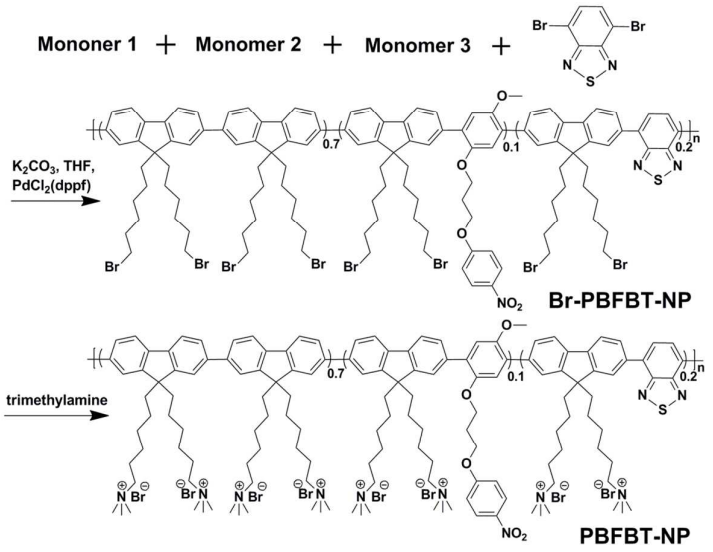

Scheme 2 The synthesis of PBFBT-NP.

As shown in Figure S1, the UV-vis absorption spectra and the fluorescence spectra of PBFBT-NP were carried out in water without the requiring of any organic solvent such as ethanol or DMSO as co-solvent, which is advantageous to application in bioanalysis.[38-40] The absorption spectra showed that PBFBT-NP has two absorption peaks at 350 nm and 430 nm, respectively. In this experiment, the excitation wavelength is set at 430 nm to avoid 350 nm UV light damaging cells and bacteria in following hypoxia diagnosis and antibacterial tests, and the emission wavelength is obtained around 558 nm in the absence of NTR. To do control experiments in following researches, we also synthesized the copolymer PBFBT devoid of p-nitrophenyl side groups. The synthesis procedure was shown in Scheme S1 and the characterizations were presented in Supporting Information. Figure S1b showed PBFBT have the similar absorption peaks at 349 and 440 nm, respectively, and emission peak at

558 nm, which indicated that the p-nitrophenyl side groups did not have much influence on the absorption and emission spectra of copolymers.

Optical Response of PBFBT-NP to NTR. As shown in Figure 1, before addition of NTR, PBFBT-NP (0.1 μM) in the presence of 100 μM NADH emitted an ultra-weak fluorescence because of PET process from backbone to p-nitrophenol in the side chain (Scheme 1). Therefore, the ultra-low fluorescence background signal enables PBFBT-NP beneficial to the highly sensitive detection of NTR. Upon addition of an aliquot of NTR, the fluorescence intensity of PBFBT-NP increased. When the concentration of NTR was added to 14.0 μg/mL, a significant enhancement of about 113-fold in fluorescence intensity was observed for PBFBT-NP (The fluorescence ratio were shown in Figure S2 in Supporting Information), which is benefit from the NTR reducing nitro into amino substance. The reason for the enhancement of fluorescence is to inhibit the PET process. Due to copolymers forming very loose aggregates in aqueous solution, it is possible that part of the nitrophenyl groups may be trapped slightly inside of the aggregates at the first. However, when NTR is added, the nitrophenyl groups still can be accessible to NTR that could change the microenvironment of copolymers, resulting in aggregates disrupting. According to the previously reported NTR-catalyzed reactions, NTR performs high reactivity to aromatic substrates due to strong interaction between them, including hydrogen bonding, π−π stacking interaction,

hydrophobic effect, and so on. The nitro groups in substrates can be reduced ultimately to an amino group,[7, 10] which contributes to the distinct fluorescence enhancement of PBFBT-NP. In Figure 1b, the fluorescence intensity in the presence and absence of NTR was recorded at 530 nm. The fluorescence increased along with the increment of NTR concentration. Moreover, we can find that this method had a wide linear range from 0 to 14.0 μg/mL. The detection limit for NTR was calculated as low as 2.9 ng/mL (LOD calculation equation was shown in Supporting Information).

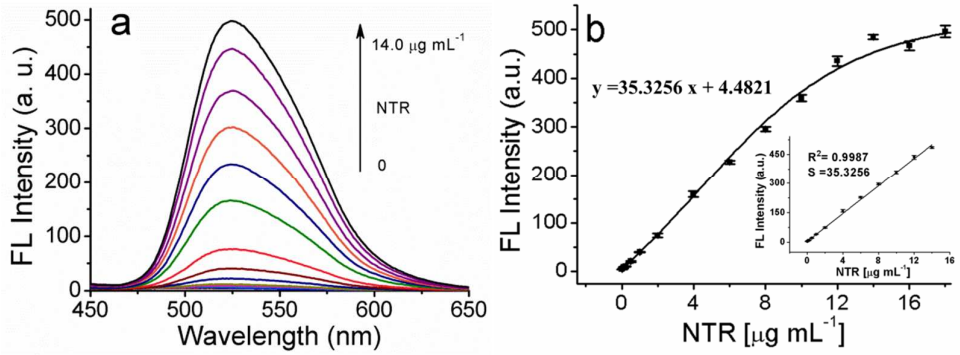

Figure 1 (a) Fluorescence spectra and (b) fluorescence intensity of PBFBT-NP (0.1 μM) after addition to different concentrations of NTR in the presence of NADH in Tris-HCl (10 mM, 7.4) (inset: linear relationship between intensity to and low NTR concentration). The error bars represent the standard deviations of three parallel measurements. λ_{ex} = 430 nm, λ_{em} =530 nm.

In addition, we carried out the control experiments of NTR test without NADH and PBFBT response to NTR. As shown in Figure S3a, no obvious fluorescence enhancement of PBFBT-NP was observed in the absence of

NADH, which presented that NADH as an electron donor plays a key role in the reduction reaction. Figure S3b showed that the fluorescence of PBFBT only increase a little in the presence of NTR and NADH because of PBFBT devoid of p-nitrophenyl side groups. These results well proved that the fluorescence enhancement of PBFBT-NP in the presence of NTR and NADH benefited from the nitro reduction into amino group by NTR. Additionally, in the presence of NTR, the emission maximum of both PBFBT-NP and PBFBT blue shifts may result from NTR disrupting the aggregates of copolymers, which leads to the conjugation change. To support the speculation, we measured the emission spectra of PBFBT-NP and PBFBT in the presence of bovine serum albumin (BSA). As shown in Figure S3, once addition of BSA in the solution of PBFBT-NP, the maximum emission of PBFBT-NP blue shifts around 10 nm, whereas that of PBFBT blue shifts about 2 nm. The tendency of maximum emission blue-shift is consistent with that induced by NTR. Therefore, the addition of enzyme may change the microenvironment of copolymers, resulting in the aggregates changing and maximum emission blue-shift.

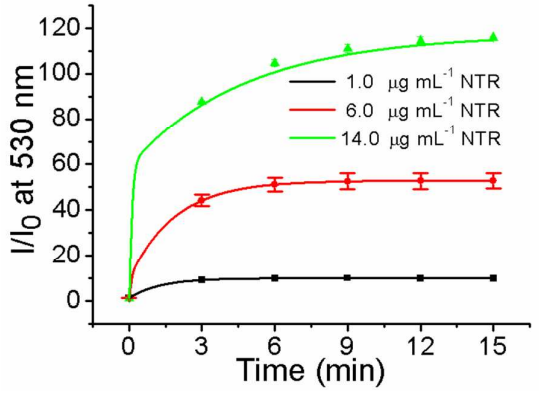

Figure 2. The fluorescence intensity ratio of PBFBT-NP (0.1 μM) with respect to the reaction time in the presence of varied concentrations of NTR. The error bars represent the standard deviations of three parallel measurements. λ_{ex} = 430 nm.

To investigate the response time, we measured the fluorescence spectra of PBFBT-NP/NADH solution, and fluorescence ratio at 530 nm was set as a function of the reaction time. First, the concentration of NTR is fixed at 14.0 μg/mL, because the activity of NTR gives the maximum response at this concentration, which is above mentioned. As shown in Figure 2, the ratio increases from around 1 to 88 quickly for the PBFBT-NP/NADH incubating with NTR for 3 min. After NTR reaction for 6 min, the ratio increases to the plateau, which demonstrates the enzymatic activity of NTR is desirable. Obviously, the same results were obtained at other concentrations of NTR, such as 1.0, 6.0 μg/mL. It should be noted that the enzyme assay is complete in a short time (6 min) without any time-consuming process. Other method reported by Ma needs 30 min to react with NTR and that reported by Li needs 10 min to reach the plateau.[2,7] Thus, our method presents a more rapid and simple assay with high sensitivity for NTR.

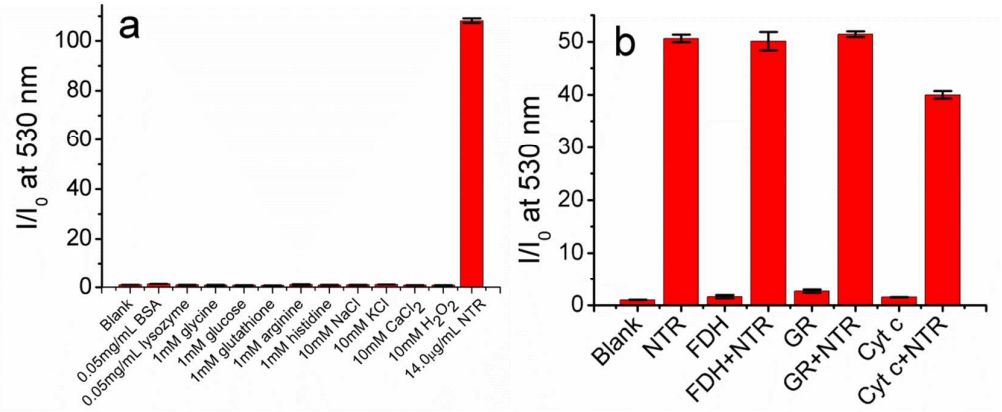

Figure 3 (a) Fluorescence ratio of PBFBT-NP after addition different kinds of potential interfering species and 14.0 μg/mL NTR in the presence of NADH in Tris-HCl; (b) Fluorescence ratio of PBFBT-NP after addition various redox species and 6.0 μg/mL NTR in the presence of NADH in Tris-HCl. FDH: formate dehydrogenase (10 μg/mL); GR: glutathione reductase (10 μg/mL); Cyt c: cytochrome c (10 μg/mL). The error bars represent the standard deviations of three parallel measurements. λ_{ex} = 430 nm.

To further study the reaction selectivity of PBFBT-NP, various potential interfering species were added respectively to PBFBT-NP (0.1 μM) solution in the presence of 100 μM NADH, such as salts (K^+, Na^+, Ca^{2+}), amino acids (glycine, arginine, histidine), glucose, reactive oxygen species (H_2O_2), lysozyme, glutathione, and BSA. As shown in Figure 3a, no apparent fluorescence enhancement was observed no matter any of the interfering species was present. However, when 14.0 μg/mL NTR was added in the same condition, the significant fluorescence signal enhancement was observed as before. Furthermore, other kinds of potential interfering species, such as

oxidoreductases (formate dehydrogenase, glutathione reductase) and electron transporters (cytochrome c), were also investigated. As depicted in Figure 3b, these electron transporters and enzymes exhibited no response to PBFBT-NP and don't interfere with the fluorescence enhancement of PBFBT-NP in the presence of NTR. Therefore, PBFBT-NP exhibits high selectivity for NTR over other species.

In addition, an inhibition test about the activity of NTR was also investigated. Dicoumarin is used usually as the inhibitor of NTR. As shown in Figure S4, when PBFBT-NP was pre-treated with 0.05 mM dicoumarin and then mixed with NTR, the fluorescence intensity is much lower than that in the absence of dicoumarin. Moreover, when the concentration of dicoumarin increased to 0.5 mM, the fluorescence intensity of PBFBT-NP was very low. The results demonstrate that increasing the concentration of dicoumarin can cause a greater decrease in fluorescence intensity. Also, the test confirmed that the fluorescence signal response of PBFBT-NP to NTR can be effectively inhibited by the inhibitor dicoumarin, and the enzyme-catalyzed reduction reaction brings the fluorescence signal enhancement response of PBFBT-NP to NTR.

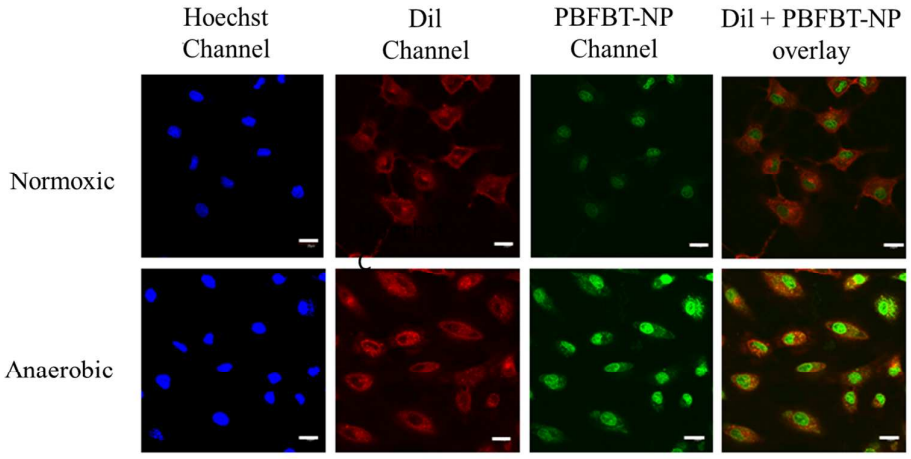

Figure 4 Confocal fluorescence microscopy images of A549 incubated with 3 μM PBFBT-NP under normoxic or anaerobic conditions. The fluorescence imaging of Hoechst (fluorescent stains for labeling DNA), Dil (cell membrane dye) and PBFBT-NP were collected at 425 - 475 nm (λ_{ex} = 405 nm), 575 - 675 nm (λ_{ex} = 559 nm), and 500 - 545 nm (λ_{ex} = 488nm), respectively. The scale bar is 20 μm.

Fluorescence Imaging of Hypoxia in A549 Cells. It is well known that the level of NTR directly corresponds with the hypoxic status, which means the decrease of O_2 level can lead to the increase of NTR concentration in tumors. As mentioned above, the nitro group in side chain of PBFBT-NP can readily be transferred into the amino group via a reduction pathway by NTR, which brings about the great enhancement of PBFBT-NP fluorescence. Thus PBFBT-NP is expected to be capable of monitoring the hypoxic degree by reacting with the endogenous NTR. To carry out the test of hypoxic tumor cells fluorescence imaging by PBFBT-NP, A549 cells was used here because they were known to

express NTR. The cells were grown under anaerobic conditions for 6 h, and then were treated with 3 μM PBFBT-NP for 1.5 h. As we can see in Figure 4, A549 cells incubated under normoxic conditions showed very weak green fluorescence background signal in nucleus. Interestingly, the cells incubated under anaerobic conditions showed very strong green fluorescence in nucleus. As mentioned before that the very loose aggregates of PBFBT-NP can be disrupted easily once the microenvironment changes. After PBFBT-NP enter inside the complex cellular environment by endocytosis, the aggregates could be disrupted then the cationic PBFBT-NP may go through nuclear pores inside cell nuclei by the electrostatic and hydrophobic interactions. The cell nuclei thus are labeled with PBFBT-NP. In addition, the control experiments of cell imaging of PBFBT were carried out according to the same procedure as PBFBT-NP. As shown in Figure S5, after incubating with PBFBT for 1.5 h no matter under normoxic conditions or under anaerobic conditions, all A549 cells showed green fluorescence signal in nucleus, which resulted from the PBFBT fluorescence emission without the requirement of NTR reduction. [34-35, 40, 44] In general, the PBFBT-NP probe can enter inside the cells by endocytosis and can be used to in cellulo imaging the hypoxic status via its reaction with the endogenous NTR.

Basically, low cell cytotoxicity at appropriate concentration is necessary for a potential fluorescent probe. Herein, the cell cytotoxicity of the PBFBT-NP was

tested using MTT assay against A549 cells. The cell viability is expressed by the ratio of the absorbance of the cells incubated with PBFBT-NP to the cells incubated with culture medium only. As shown in Figure S6, the cell viability remained at ~100% even if the concentration of PBFBT-NP was 10.0 μM after incubation for 48 h. These results showed that PBFBT-NP with such low cell cytotoxicity has greatly potential application as fluorescent probe for cell imaging and future biological analysis application.

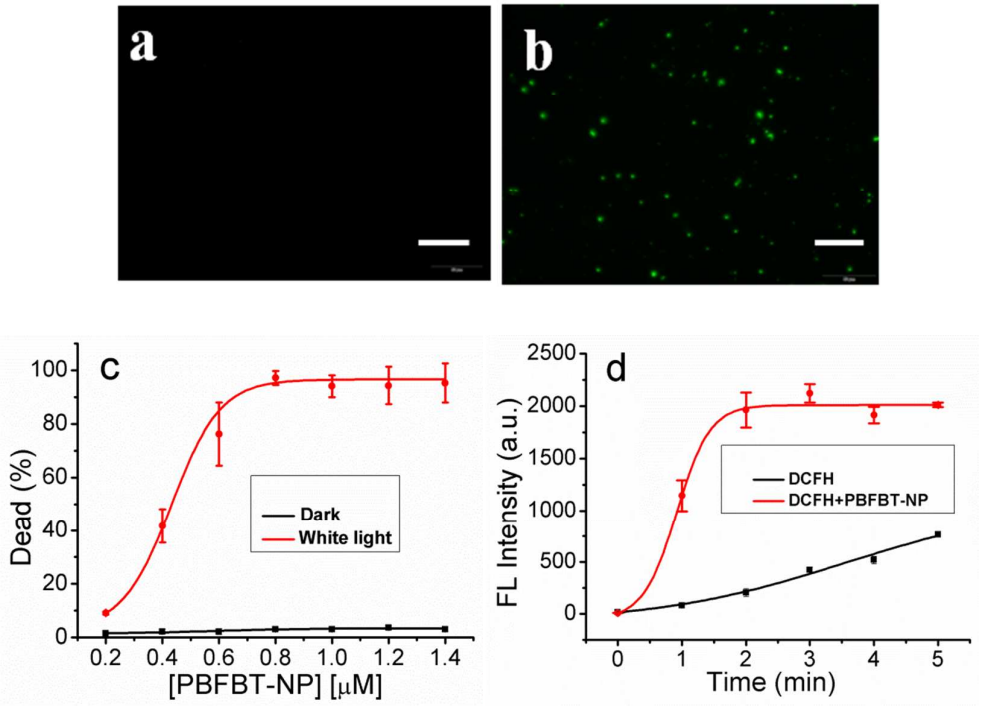

Figure 5 Fluorescence imaging of *E. coli* incubated without PBFBT-NP (a) and with PBFBT-NP (b) for 30 min. Scale bar = 50 μm. (c) *E. coli* viability against PBFBT-NP at various concentrations for 60 min under white light. (d) PBFBT-NP sensitized ROS upon

white light irradiation with an excitation of 488 nm. The error bars represent the standard deviations of three parallel measurements.

Bacteria Imaging and Antibacterial Performance of PBFBT-NP. Taking advantage of PBFBT-NP probe sensing NTR with sensitivity, rapidity and low cytotoxicity, other NTR-related analysis, such as microbial imaging and antibacterial activity were also investigated based on this new probe. It is reported that the NTR is expressed commonly in microorganisms, such as *Escherichia coli*. As mentioned above, the PBFBT-NP probe can clearly detect the endogenous NTR and image the hypoxic tumor cells. Correspondingly, the PBFBT-NP is anticipated to apply for microbial imaging that usually need expensive commercial dyes. The *E. coli* cells imaging tests were carried out as followed: PBFBT-NP (5 μM) was added to bacterial suspension (2×10^7 mL^{-1}) and then the mixture was incubated for half an hour at 37 ^oC in the shaker. *E. coli* bacteria then were observed under inverted fluorescence microscope without any commercial dye staining. As shown in Figure 5a and 5b, the bacteria are non-blooming without PBFBT-NP probe, however, in the presence of PBFBT-NP, the bacteria emit bright green fluorescence. These data indicated that the nitro group of PBFBT-NP was reduced to the amine group by NTR in *E. coli* and the recovered fluorescence of PBFBT-NP can be used to image bacteria. In addition, the control experiment of *E. coli* cells imaging after incubating with PBFBT-NP and dicoumarin were carried out. As shown in

Figure S7, in the presence of dicoumarin, almost no bacteria emit green fluorescence due to the dicoumarin inhibiting the NTR activity inside the bacteria cells. Therefore, the nitro group of PBFBT-NP can't be reduced to the amine group by NTR, leading to *E. coli* no blooming. The results proved that the probe should enter the bacteria first and then be reduced by NTR.

Based on the microbial imaging, anti-bacteria test was further carried out by flow cytometry. Recent researches indicated cationic conjugated polymers (CCPs) possess high antibacterial activities and can be used as photosensitizer for photodynamic therapy.[30, 52-55] The PBFBT-NP is one of typical CCPs, and also can be considered as a PDT agent for antibacterial. As shown in Figure 5c (Complementary flow cytometry data were shown in Figure S8), the red line represents the mixture solution contained PBFBT-NP and *E.coli* (2×10^7 mL^{-1}) was exposed to white light for 60 min. The black line shows that the mixture solution contained PBFBT-NP and *E.coli* was incubated in dark for 60 min. Under white light irradiation, the antibacterial activities of PBFBT-NP showed the concentration-dependent response. When the concentration of PBFBT-NP was 0.4 μM, over 40% *E. coli* bacteria were dead. Interestingly, when the concentration of probe is 0.8 μM, the disinfection efficiency can reach up to near 100% under white light. The corresponding fluorescence images were obtained in the presence of PBFBT-NP and propidium iodide (PI, red fluorescence for dead bacteria). As shown in Figure S9, green indicates live

bacteria, red indicates dead bacteria, and orange represents the dying bacteria. The orange and red bacteria cells were observed more and more along with the increasing of PBFBT-NP concentration, which means more and more *E. coli* bacteria were killed by PBFBT-NP under white light irradiation. The results are highly consistent with that obtained by flow cytometry.

To prove that the antibacterial effect should result from reactive oxygen species produced by PBFBT-NP with white irradiation, we utilized 2,7-dichlorofluorescein diacetate (DCFH-DA) as a cell-permeable fluorogenic ROS-sensitive probe in our experiment. As shown in Figure 5d, an apparent emission at 525 nm was detected upon irradiating DCFH with white light in the presence of PBFBT-NP, while the control without PBFBT-NP emits weak fluorescence, which confirm the efficient generation of ROS by PBFBT-NP. These results indicate that the PBFBT-NP also can be used as a good antibacterial photosensitizer.

CONCLUSIONS

In summary, we have designed a new cationic conjugated polymer PBFBT-NP as fluorescent probe that not only can be applied to conveniently detect the NTR level and hypoxia status of tumor cells, but also can be applied to bacteria imaging and highly efficient anti-bacterial. The nitro group as NTR capturing group was introduced into the probe, which afforded a very low fluorescence

background due to the PET process from the backbones of probe to the side chains. The study in this paper also verified that PBFBT-NP probe exhibited rapidity, simplicity, high selectivity and sensitivity to NTR. More importantly, the in cellulo hypoxia status of tumor cells can be visualized by the greatly enhanced fluorescence of PBFBT-NP through endogenous NTR reduction reaction. In addition, the probe can be used for microbial imaging instead of commercial stain dyes which are usually expensive. Interestingly, the probe presented about 100% antibacterial activity against *E. coli* at low concentration with white light irradiation. All the above features demonstrate that the new multifunctional probe is promising for widespread use in NTR-related biological analysis.

ASSOCIATED CONTENT

Supporting Information. Detailed synthesis procedure of PBFBT, other experimental procedures and figures as noted in text. This material is available free of charge via the Internet at http://pubs.acs.org.

AUTHOR INFORMATION

Corresponding Author

*Phone: (086) 29-81530844. Fax: (086) 29-81530727. E-mail: yltang@snnu.edu.cn.

Notes

The authors declare no competing financial interest.

ACKNOWLEDGEMENTS

We are grateful for the financial support from the National Natural Science Foundation of China (Grants 21675106, 21222509, 21335005), the 111 Project (B14041), Program for Changjiang Scholars and Innovative Research Team in University (IRT 14R33), and the Program for Innovative Research Team in Shaanxi Province (No. 2014KCT-28).

REFERENCES

(1) Wilson, W. R.; Hay, M. P. *Nat. Rev. Cancer* **2011**, *11*, 393-410.

(2) Li, Z.; Li, X. H.; Gao, X. H.; Zhang, Y. Y.; Shi, W.; Ma, H. M. *Anal. Chem.* **2013**, *85*, 3926-3932.

(3) Chen, Y.; Hu, L. Q. *Med. Res. Rev.* **2009**, *29*, 29-64.

(4) Brown, J. M.; Wilson, W. R. *Nat. Rev. Cancer* **2004**, *4*, 437-447.

(5) Tang, Y.; Lu, A.; Aronow, B. J.; Wagner, K. R.; Sharp, F. R. *Eur. J. Neurosci.* **2002**, *15*, 1937-1952.

(6) Murdoch, C.; Muthana, M.; Lewis, C. E. *J. Immunol.* **2005**, *175*, 6257-6263.

(7) Li, Y.; Sun, Y.; Li, J.; Su, Q.; Yuan, W.; Dai, Y.; Han, C.; Wang, Q.; Feng W.; Li. F. *J. Am. Chem. Soc.* **2015** *137*, 6407-6416.

(8) Gladwin, M. T.; Raat, N. J.; Shiva, S.; Dezfulian, C.; Hogg, N.; Kim-Shapiro, D. B.; Patel, R. P. *Am. J. Physiol. Heart. Circ. Physiol.* **2006**, *291*, H2026-2035.

(9) Crawford, J. H.; Isbell, T. S.; Huang, Z.; Shiva, S.; Chacko, B. K.; Schechter, A. N.; Darley-Usmar, V. M.; Kerby, J. D.; Lang Jr, J. D.; Kraus, D.; Ho, C.; Gladwin, M.

T.; Patel, R. P. *Blood* **2006**, *107*, 566-574.

(10) Xu, G.; McLeod, H. L. *Clin. Cancer. Res.* **2001**, *7*, 3314-3324.

(11) Searle, P. F.; Chen, M. J.; Hu, L.; Race, P. R.; Lovering, A. L.; Grove, J. I.; Guise, C.; Jaberipour, M.; James, N. D.; Mautner, V.; Young, L. S.; Kerr, D. J.; Mountain, A.; White, S. A.; Hyde, E. I. *Clin. Exp. Pharmacol. Physiol.* **2004**, *31*, 811-816.

(12) Guo, T.; Cui, L.; Shen, J.; Zhu, W.; Xu, Y.; Qian, X. *Chem. Commun.* **2013**, *49*, 10820-10822.

(13) Grove, J. I.; Lovering, A. L.; Guise, C.; Race, P. R.; Wrighton, C. J.; White, S. A.; Hyde; E. I.; Searle, P. F. *Cancer Res.* **2003**, *63*, 5532-5537.

(14) Denny, W. A. *Curr. pharm. Design* 2002, **8**, 1349-1361.

(15) Berne, C.; Betancor, L.; Luckarift, H. R.; Spain, J. C. *Biomacromolecules* **2006**, *7*, 2631-2636.

(16) Symons, Z. C.; Bruce, N. C. *Nat. Prod. Rep.* **2006**, *23*, 845-850.

(17) Roldan, M. D.; Perez-Reinado, E.; Castillo. F.; Moreno-Vivian, C. *FEMS Microbiol. Rev.* **2008**, *32*, 474-500.

(18) Nguyen-Tran, H. H.; Zheng, G. W.; Qian, X. H.; Xu, J. H. *Chem. Commun.* **2014**, *50*, 2861-2864.

(19) Zhang, J.; Liu, H. W.; Hu, X. X.; Li, J.; Liang, L. H.; Zhang, X. B.; Tan, W. *Anal. Chem.* **2015**, *87*, 11832-11839.

(20) Xu, K. H.; Wang, F.; Pan, X. H.; Liu, R. P.; Ma, J.; Kong, F. P.; Tang, B. *Chem. Commun.* **2013**, *49*, 2554-2556.

(21) Shi, Y.; Zhang, S.; Zhang, X. *Analyst* **2013**, *138*, 1952-1955.

(22) Mukherjee, A.; Rokita, S. E. *J. Am. Chem. Soc.* 2015, **137**, 15342-15345.

(23) Dai, C.; Yang, D.; Zhang, W.; Bao, B.; Cheng, Y.; Wang, L. *Polym. Chem.* **2015**, *6*, 3962-3969.

(24) Cui, L.; Zhong, Y.; Zhu, W. P.; Xu, Y. F.; Du, Q. S.; Wang, X.; Qian, X. H.; Xiao, Y. *Org. Lett.* **2011**, *13*, 928-931.

(25) Yuan, J. Y.; Xu, Y. Q.; Zhou, N. N.; Wang, R.; Qian, X. H. *RSC Adv.* **2014**, *4*, 56207-56210.

(26) Xue, C.; Lei, Y. J.; Zhang, S. C.; Sha, Y. W. *Anal. Methods* **2015**, *7*, 10125-10128.

(27) Huang, H. C.; Wang, K. L.; Wang, S. T.; Lin, S. Y.; Lin, C. M. *Biosens. Bioelectron.* **2011**, *26*, 3511-3516.

(28) Su, J. C.; Guise, C. P.; Wilson, W. R. *Biochem. J.* **2013**, *452*, 79-86.

(29) Zhu, C. L.; Yang, Q.; Liu, L. B.; Wang, S. *Angew. Chem. Int. Ed.* **2011**, *50*, 9607-9610.

(30) Zhu, C. L.; Liu, L.; Yang, Q.; Lv, F. T.; Wang, S. *Chem. Rev.* **2012**, *112*, 4687-4735.

(31) Thomas, S. W.; Joly, G. D.; Swage, T. M. *Chem. Rev.* **2007**, *107*, 1339−1386.

(32) Wosnick, J. H.; Mello, C. M.; Swager, T. M. *J. Am. Chem. Soc.* **2005**, *127*, 3400−3405.

(33) Dwight, S. J.; Gaylord, B. S.; Hong, J. W.; Bazan, G. C. *J. Am. Chem. Soc.* **2004**, *126*, 16850−16859.

(34) Wang, C.; Tang, Y. L.; Liu, Y.; Guo, Y. *Anal. Chem.* **2014**, *86*, 6433-6438.

(35) Wang, C.; Tang, Y. L.; Guo, Y. *ACS Appl. Mater. Interfaces* **2014**, *6*,

21686-21691.

(36) Satrijo, A.; Swager, T. M. *J. Am. Chem. Soc.*, **2007** *129*, 16020-16028.

(37) Ho, H. A.; Najari, A.; Leclerc, M. *Acc. Chem. Res.* **2008**, *41***,** 168−178.

(38) Zhang, J. Y.; Xing, B. L.; Song, J. Z.; Zhang, F.; Nie, C. Y.; Jiao, L.; Liu, L. B.; Lv, F. T.; Wang, S. *Anal. Chem.* **2014**, *86*, 346-350.

(39) Song, J. Z.; Zhang, J. Y.; Lv, F. T.; Cheng, Y. Q.; Wang, B.; Feng, L. H.; Liu, L. B.; Wang, S. *Angew. Chem. Int. Ed.* **2013**, *52*, 13020-13023.

(40) Liu, B.; Bazan, G. C. *Nat. Protoc.* **2006**, *1*, 1698-1702.

(41) Tang, Y. L.; Liu, Y.; Cao, A. *Anal. Chem.* **2013** *85*, 825-830.

(42) Pinto, M. R.; Schanze, K. S. *Proc. Natl. Acad. Sci. USA* **2004**, *101*, 7505-7510.

(43) Liu, X. F.; Fan, Q. L.; Huang, W. *Biosens. Bioelectron.* **2011**, *26*, 2154-2164.

(44) He, F.; Tang, Y. L.; Yu, Y. M.; Feng, F. D.; An, L. L.; Sun, H.; Wang, S.; Li, Y. L.; Zhu, D. B.; Bazan, G. C. *J. Am. Chem. Soc.* **2006**, *128*, 6764-6765.

(45) Feng, F. D.; Tang, Y. L.; Wang, S.; Li, Y. L.; Zhu, D. B. *Angew. Chem. Int. Ed.* **2007**, *46*, 7882-7886.

(46) Wang, R.; Yu, F. B.; Chen, L. X.; Chen, H.; Wang, L. J.; Zhang, W. W. *Chem. Commun.* **2012**, *48*, 11757-11759.

(47) Meng, L. B.; Li, D. Q.; Xiong, S. H.; Hu, X. Y.; Wang, L. Y.; Li, G. G. *Chem. Commun.* **2015**, *51*, 4643-4646.

(48) Pu, K. Y.; Fang, Z.; Liu, B. *Adv. Funct. Mater.* **2008**, *18*, 1321-1328.

(49) Zhou, Z. J.; Corbitt, T. S.; Parthasarathy, A.; Tang, Y. L.; Ista, L. F.; Schanze, K. S.; Whitten, D. G. *J. Phys. Chem. Lett.* **2010**, *1*, 3207-3212.

(50) Liu, B.; Bazan, G. C. *J. Am. Chem. Soc.*, **2004** *126*, 1942-1943.

(51) Feng, L. H.; Liu, L. B.; Lv, F. T.; Bazan, G. C.; Wang, S. *Adv. Mater.* **2014**, *26*, 3926-3930.

(52) Bai, H. T.; Yuan, H. X.; Nie, C. Y.; Wang, B.; Lv, F. T.; Liu, L. B.; Wang, S. *Angew. Chem. Int. Ed.* **2015**, *54*, 13208-13213.

(53) Lu, L. D.; Rininsl, F. H.; Wittenburg, S. K.; Achyuthan, K. E.; McBranch, D.W.; Whitten, D. G.. *Langmuir* **2005**, *21*, 10154-10159.

(54) Tew, G. N.; Scott, R. W.; Klein, M. L.; Degrado, W. F. *Acc. Chem. Res.* **2010**, *43*, 30-39.

(55) Yuan, H. X.; Wang, B.; Lv, F. T.; Liu, L. B.; Wangm S. *Adv. Mater.* **2014**, *26*, 6978-6982.

For TOC only

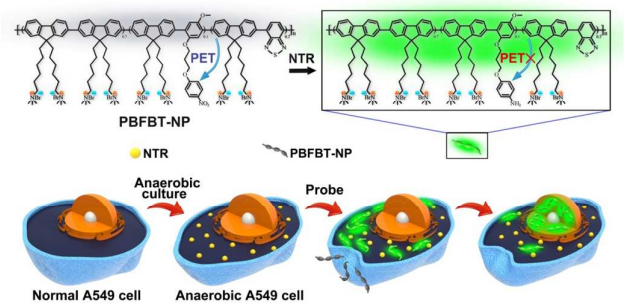
PET
NTR
PETX
PBFBT-NP
NTR
PBFBT-NP
Anaerobic culture
Probe
Normal A549 cell
Anaerobic A549 cell